Characterization of HcaA, a novel autotransporter protein in *Helicobacter cinaedi*, and its role in host cell adhesion

Short title: *Helicobacter cinaedi* autotransporter HcaA

Sae Aoki[1], Shigetarou Mori[1], Hidenori Matsui[1], Keigo Shibayama[2], Tsuyoshi Kenri[1], Emiko Rimbara[1*]

[1]Department of Bacteriology II, National Institute of Infectious Diseases, Tokyo, Japan

[2]Department of Bacteriology, Nagoya University Graduate School of Medicine, Nagoya, Aichi, Japan

***Corresponding author:**

Emiko Rimbara

Department of Bacteriology II, National Institute of Infectious Diseases

4-7-1 Gakuen, Musashimurayama-shi, Tokyo 208-0011, JAPAN

Tel: +81-42-561-0771

Email: rimbara@niid.go.jp

ABSTRACT

Helicobacter cinaedi infects the human gut and causes invasive infections such as bacteremia and cellulitis by bacterial translocation. However, how *H. cinaedi* attaches to host cells and establishes infection has not been elucidated. In this study, we focused on a novel autotransporter protein, i.e., *H. cinaedi* autotransporter protein A (HcaA) to examine its relationship with *H. cinaedi* pathogenicity. The cytotoxicity of *H. cinaedi* infection in the colon epithelial cell lines (Caco-2 and HT-29) by lactate dehydrogenase assay showed a significant reduction in cytotoxicity by HcaA knockout. Adhesion assays further revealed that the HcaA-knockout strain showed significantly reduced attachment of *H. cinaedi* to the human epithelial colorectal adenocarcinoma cell line (Caco-2) compared to the wild-type strain. To determine the role of HcaA in *H. cinaedi* infection *in vivo*, *H. cinaedi* wild-type and HcaA-knockout strains were orally infected C57BL/6 mice. The colonized bacteria were then measured 7, 14, and 28-days post-infection. The number of colonized *H. cinaedi* cells was significantly lower in HcaA-knockout strain infections than in wild-type strain infections at 7 days post-infection. Recombinant HcaA protein showed strong adhesion characteristics to the human monocytic cell line (U937) by adhesion assay used recombinant purified HcaA protein. The adherent activity was diminished by the replacement of the RGD motif in HcaA with RAD, indicating the contribution of the RGD motif in HcaA to host cell adherence. These results suggest that HcaA, a novel autotransporter protein in *H. cinaedi*, plays a significant role in establishing infection as an adhesin.

Keywords: *Helicobacter cinaedi*, autotransporter protein, type V secretion system, non-*Helicobacter pylori Helicobacter* species, cell adhesion

IMPORTANCE

Helicobacter species are classified as gastric or enterohepatic according to their habitat. Enterohepatic *Helicobacter* species inhabit the intestine, colon and liver; among them, *H. cinaedi* has been most frequently isolated from humans. *H. cinaedi* commonly causes bacteremia and cellulitis in immunocompromised hosts. Here, we focused on the *H. cinaedi* autotransporter protein A (HcaA), a novel virulence factor in *H. cinaedi*. We discovered that HcaA contributed to cell adhesion via its RGD motif. Furthermore, in animal experiments, the number of colonized bacteria was decreased in HcaA knockout strain infections, supporting the hypothesis that HcaA contributes to the adhesion of *H. cinaedi* to host cells. Our study provides a novel mechanism for the establishment of *H. cinaedi* infections and is expected to provide new insights into the role of autotransporter proteins in the establishment of *Helicobacter* species infection.

INTRODUCTION

Helicobacter species, gram-negative and helical bacilli, are isolated from humans and mammals such as dogs, cats, pigs, and birds. They are grouped into gastric or enterohepatic *Helicobacter* species according to their habitat. *Helicobacter pylori*, a typical gastric *Helicobacter* species, is a pathogenic bacterium that infects the human stomach and is a major cause of gastric cancer (1).

Among enterohepatic *Helicobacter* species, *H. cinaedi* is the most frequently isolated strain from humans. This strain is mainly isolated from patients with bacteremia in immunocompromised hosts. *H. cinaedi* is known to cause recurrent cellulitis, and in recent years, it has been reported to cause an infected aortic aneurysm, subdural hematoma, and hepatic cyst infections (2–6). The first isolation of *H. cinaedi* was reported in a homosexual man with intestinal symptoms in Seattle in 1984, and the first isolation in Japan was reported

66 in 2003 (7,8). For unknown reasons, *H. cinaedi* infection is mainly reported in Japan,
67 followed by several case reports from Denmark (9,10). A retrospective study in a single
68 hospital in Japan indicated that, of all blood culture-positive samples, 2.2% (126/5,769 sets of
69 blood cultures) became *H. cinaedi*-positive when the period of blood culture was extended,
70 indicating that *H. cinaedi* infections may be overlooked in other countries (11).

71 Cytolethal distending toxin (CDT) is a virulence factor in *H. cinaedi*. CDT is composed of
72 three polypeptide subunits encoded by CdtA, CdtB and CdtC (12,13). Among these proteins,
73 CdtB has function of nuclease activity and cause DNA damage. As a result, the host cells
74 were led to cell senescence and apoptosis. CdtA and CdtC play a role in delivering CdtB into
75 host cells. Another virulence factor *H. cinaedi* antigen CAIP contributes atherosclerosis
76 inflammation by the differentiation and maintenance of the pro-inflammatory profile of
77 human macrophages and triggers the formation of foam cells (14). However, the mechanism
78 by which *H. cinaedi* establishes infection has not been fully elucidated.

79 Autotransporter proteins (ATs) are type V secretion systems (T5SS) that consist of a
80 passenger domain, which plays a significant role, a functional secreted portion, and an
81 autotransporter domain involving a β-barrel, which exports the passenger domain from the
82 periplasm to the extracellular environment. ATs are widely found in gram-negative bacteria
83 and have diverse functions in their pathogenesis, acting as toxins and adhesion factors (15).
84 For example, the vacuolating cytotoxin A (VacA) of *H. pylori* is an ATs that acts as a toxin
85 contributing *to H. pylori* pathogenesis by inducing vacuolation in the host cells, altering
86 mitochondrial membrane permeability and apoptosis, and stimulation of pro-inflammatory
87 signaling (16). *H. pylori* possesses three other autotransporter proteins, ImaA, VlpC, and
88 FaaA, which contribute to establishing infection and motility (17). In *H. cinaedi*, one
89 autotransporter protein is encoded in its chromosome, which has not previously been

90 characterized. In this study, we named this uncharacterized protein *H. cinaedi* autotransporter
91 protein A (HcaA) and investigated its contribution to *H. cinaedi* pathogenicity.
92
93 **RESULTS**
94 **HcaA knockout strain showed reduced cytotoxicity and adherence and did not invade**
95 **human colon epithelial cells *in vitro***
96 We constructed deletion knockout mutants of *hcaA* gene. HcaA is a 197 kDa protein
97 encoded by the 5,478 bp *hcaA* gene. A donor fragment containing an antibiotic selection
98 marker (*aphA* gene) flanked by a paralog sequence approximately 1,000 bp upstream and
99 downstream of *hcaA* was created (Fig. 1A, upper and middle). *H. cinaedi* MRY12-0027 and
100 MRY08-1234 strains were used as host strains, and *hcaA* was knocked out by replacing *hcaA*
101 with *aphA* by paralog recombination (Fig. 1A, bottom). Knockout of *hcaA* was verified by
102 polymerase chain reaction (PCR) amplification and immunoblot analysis (Fig. 1B and C). The
103 results of immunoblot analysis suggested that HcaA was localized in the membrane fraction
104 (Fig. 1C).
105 The effects of the HcaA-knockout strain on cellular cytotoxicity were evaluated *in vitro*
106 using a lactate dehydrogenase (LDH) assay. When the human epithelial colorectal
107 adenocarcinoma (Caco-2) cell line and human colon cancer (HT29) cell line were infected
108 with *H. cinaedi*, LDH production in cells infected with the HcaA-knockout strain was
109 significantly lower than that of the wild-type strain (Fig. 2A). Therefore, HcaA may play a
110 significant role in the cytotoxic effects of *H. cinaedi* infection on the epithelial cells. HcaA
111 knockout did not affect LDH production when mucus-secreting HT29-MTX cells were used
112 (Fig. 2A). This suggests mucin's protective role in reducing the cytotoxicity caused by *H.*
113 *cinaedi* was not affected by the knockout of HcaA.

114 To determine whether HcaA contributes to cell adhesion and invasion, we performed a
115 gentamicin assay, and compared the rate of adherents and invaded *H. cinaedi* cells between
116 the wild-type and knockout strains. The adhesion rate of *H cinaedi* MRY12-0027 strain to
117 Caco-2 cells was significantly decreased by HcaA knockout (Fig. 2B, upper panel). A
118 significant reduction in the adhesion rate was also observed when *H. cinaedi* MRY08-1234
119 was used (Fig. 2B, bottom panel). The invasion rate of MRY12-0027 and MRY08-1234 was
120 also reduced by HcaA knockout. However, no significant difference was observed (Fig. 2C).
121 In contrast, the invasion rate of adherent bacteria was higher in the HcaA-knockout strain (Fig.
122 2D).
123
124 **HcaA effects on the establishment of *H. cinaedi* infection in mice**
125 To clarify the role of HcaA in *H. cinaedi* infection *in vivo*, C57BL/6 female mice were
126 orally infected with *H. cinaedi* wild-type and HcaA-knockout strains. The recovery of *H.*
127 *cinaedi* from cecal contents, colon, biceps femoris muscle, trapezius muscle, and heart was
128 analyzed at 7, 14, and 28 days post-infection (Fig. 3A). As *H. cinaedi* is known as a causative
129 agent of cellulitis and infected aortic aneurysm (18), muscle and heart samples were also
130 taken in addition to the intestinal tract samples. To confirm the infection, antibody titers
131 against *H. cinaedi* in mouse serum were measured. An increase in antibody titers against
132 whole cells of *H. cinaedi* was observed in both groups of mice infected with the wild-type
133 strain and HcaA knockout strain. The antibody titers against *H. cinaedi* at 28 days post-
134 infection were significantly higher in the group of mice infected with the wild-type strain than
135 in the mice infected with the knockout strain ($P < 0.01$, Fig. 3B). Using the culture method, *H.*
136 *cinaedi* was recovered from the colon and cecal contents in both groups of mice infected with
137 the wild-type strain and HcaA-knockout strain. The recovery rate of *H. cinaedi* in cecal
138 contents was significantly higher in mice infected with the wild-type strain (4/5, 80%) than in

139 mice infected with the HcaA-knockout strain at 7 days post-infection (0/6, 0%, $P < 0.01$,
140 Table 1). Interestingly, *H. cinaedi* was detected in muscle only in the group of mice infected
141 with the wild-type strain at 7 and 28 days post-infection (Table 1). *H. cinaedi* was detected in
142 the cecal contents of all *H. cinaedi*-infected mice by quantitative real-time PCR (qPCR).
143 Bacterial cells in the cecal contents from mice infected with the HcaA-knockout strain were
144 significantly fewer than those from mice infected with the wild-type strain at 7 days post-
145 infection ($P <0.05$, Fig. 3C). At 14 and 28 days post-infection, there was a trend toward fewer
146 bacterial cells in mice infected with the HcaA-knockout strain. However, no significant
147 differences were observed between groups ($P = 0.15$ and 0.42, respectively). The reduction in
148 the number of HcaA-knockout bacterial cells was also observed through immunofluorescence
149 analysis of the colon infected with *H. cinaedi* using an anti-*H. cinaedi* antibody (Fig. 3D). *H.*
150 *cinaedi* was observed in the mucosal epithelium regardless of the presence or absence of
151 HcaA and the duration of infection; however, the number of bacteria tended to be lower in
152 samples from mice infected with the HcaA-knockout strain than in samples from mice
153 infected with the wild-type strain.
154
155 **Adhesive ability was reduced in the mutant HcaA recombinant protein**
156 The HcaA protein of *H. cinaedi* MRY 08-1234 [1,835 amino acids (aa), 197 kDa] is
157 predicted to be structured with a signal peptide (1–27 aa), passenger domain (27–1425 aa),
158 and β-barrel domain (1426–1825 aa). HcaA of *H. cinaedi* contains an Arg–Gly–Asp (RGD)
159 motif at amino acid positions 348–350. To understand the contribution of the RGD motif to
160 adhesion, a recombinant protein of the passenger region of HcaA of MRY08-1234 (WT
161 HcaA) and mutant HcaA (with the RGD motif replaced by RAD) was created (Fig. 4A). The
162 ability of the cells to adhere to U937 cells was compared between WT HcaA and mutant
163 HcaA. Mutant HcaA revealed a significant reduction in binding to U937 cells compared to

164 WT HcaA ($P < 0.05$), indicating the role of the RGD motif in binding to host cells (Fig. 4B).
165 Structural prediction of HcaA of MRY08-1234 by AlphaFold2 indicated that the RGD motif
166 of HcaA is located on the surface of the protein, supporting the contribution of the RGD motif
167 to the adherence function of HcaA in *H. cinaedi* (Fig. 4C, left). The RGD motif was
168 conserved in all *H. cinaedi* strains registered at the National Center for Biotechnology
169 Information (NCBI), including clinical isolates (Fig. S1). HcaA paralogs have been in *H. bilis*,
170 *H. fennelliae*, *H. canicola*, and *H. canis*, which are all related to *H. cinaedi* (19–21). The
171 structural predictions of HcaA paralogs by AlphaFold2 suggested that HcaA and its paralogs
172 had structural similarities in the passenger region; however, the RGD motif was present only
173 in HcaA of *H. cinaedi* (Fig. 4C and D). In addition, the HcaA paralogs had a structure
174 protruding from the surface, similar to the RGD motif of HcaA. However, the protruding
175 structure did not contain the RGD motif (Fig. 4C).
176
177 **DISCUSSION**
178 Enterohepatic *Helicobacter* species are increasingly being recognized as critical
179 mammalian pathogens. Among these, *H. cinaedi* has been reported to cause bacteremia,
180 cellulitis, and infected aortic aneurysms in humans (2,4,22). Although *H. cinaedi* infections
181 have rarely been reported, *H. cinaedi* infection cases in Japan have been increasing since 2003
182 (8,11,22). *H. cinaedi* infections have been reported to show diverse pathologies; however,
183 knowledge concerning the virulence factors of *H. cinaedi* is limited. ATs have various
184 functions that contribute to the establishing infections by pathogenic gram-negative bacteria.
185 In this study, we found that HcaA, the only ATs in *H. cinaedi*, is responsible for adhesion to
186 host cells and contributes to the pathogenesis of *H. cinaedi*. This is the first report to elucidate
187 the role of ATs in enterohepatic *Helicobacter* species.

188 Based on their protein architecture, T5SS proteins are classified into subgroups labelled
189 Va–Ve; this does not reflect the functions of the secreted passengers. Pertactin produced by
190 *Bordetella pertussis* is classified as a type Va ATs; it contributes to adhesion to cell surfaces
191 and receptors (24). VacA produced by *H. pylori* is likewise classified as a type Va AT; it
192 binds to host cells and is internalized, causing vacuolation characterized by the accumulation
193 of large vesicles (16). Serine protease autotransporters of *Enterobacteriaceae* (SPATEs)
194 produced by *Enterobacteriaceae* are also classified as type Va ATs (23). The effect of
195 SPATEs on cells varies, with the primary reported function being protease activity that
196 cleaves host proteins. HcaA is structurally similar to EspP, one of the SPATEs in *Escherichia*
197 *coli*. We tested protease activity against casein and pepsin, the major substrates for SPATEs;
198 however, no protease activity against these proteins was observed (Fig. S2A and B). In
199 contrast, the number of bacterial cells adhered to human epithelial cells and cytotoxicity
200 levels were significantly decreased by HcaA knockout. These results indicate that the
201 reduction in cytotoxicity in the HcaA knockout strain is due to the decrease in the number of
202 attached *H. cinaedi* cells and that HcaA itself may not be cytotoxic.
203 The mouse infection experiment also supported the *in vitro* data, showing that HcaA
204 knockout reduces the number of infected bacterial cells in the cecal contents of *H. cinaedi*-
205 infected mice at 7 days post-infection. Because the number of bacterial cells was comparable
206 between the wild-type and HcaA-knockout strains after 28 days of infection, HcaA could be
207 involved in cell adhesion and may play a significant role in the established phase of *H.*
208 *cinaedi* infection. Recovery of *H. cinaedi* from cecal contents and biceps femoris muscle at 7
209 days post-infection was only observed in mice infected with the wild-type strain, suggesting
210 that HcaA contributes to the establishment of *H. cinaedi* infection. Further studies are needed
211 in terms of bacterial translocation, as isolates from muscle suggested that it may be associated
212 with cellulitis caused by *H. cinaedi*. Interestingly, HcaA knockout did not affect the number

213 of invaded bacterial cells/total number of infected bacterial cells. In contrast, the number of
214 invaded bacterial cells/adhered bacterial cells increased with HcaA knockout (Fig. 2D). ATs
215 have been found to have a variety of functions. For example, ImaA, an AT in *H. pylori,* has
216 been reported to be an essential factor for host colonization and to reduce host inflammatory
217 responses by modulating the host inflammatory response by controlling the expression of
218 inflammatory cytokines IL-8 and TNF-α (25). In addition, EspC, an SPATEs, has been
219 reported to degrade various host proteins, such as hemoglobin and mucin, and also to prevent
220 cytotoxicity during the initial stage of bacterial infection by regulating pore formation (23,26).
221 Thus, HcaA may have a similar function in escaping from the host immune mechanism to
222 contribute to the establishment of chronic *H. cinaedi* infections in humans. Further analysis is
223 needed to elucidate additional functions of HcaA other than cell adhesion.

224 HcaA contains an RGD motif in its passenger region. The RGD motif acts as the
225 fibronectin cell adhesion site and plays a role in adhesion to host epithelial cells expressing
226 receptors of the RGD motif, such as integrins. Cell adhesion experiments using purified HcaA
227 with the RGD motif and mutant HcaA with the RAD motif showed that adhesion ability
228 decreased significantly upon replacing RGD with RAD. Structural prediction of the HcaA
229 structure indicated that the RGD motif is located on the surface of the protein and that the
230 motif is located at an externally protruding site. The RGD motif is known to bind to integrins,
231 and it is assumed that integrins mediate the adhesion of HcaA to cells. Our results strongly
232 suggest that the RGD motif of HcaA plays a role in cell adhesion. However, the adhesion
233 ability of HcaA was not completely diminished by replacing RGD with RAD. Therefore,
234 HcaA possibly functions as an adhesin regardless of the RGD motif, and the presence of the
235 RGD motif enhances its ability to attach to cells. HcaA paralogs are also found in
236 enterohepatic *Helicobacter* species, such as *H. bilis*, *H. canis*, *H. fennelliae,* and *H. canicola.*
237 However, none of these have an RGD motif (Fig. 4). In addition, the RGD motif of HcaA was

238 highly conserved among *H. cinaedi* strains, regardless of the origin of the strains (Fig. S1). *H.*
239 *canicola* was formerly identified as *H. cinaedi* and is genetically closest to *H. cinaedi* among
240 *Helicobacter* species (21). However, phylogenetic analysis of HcaA indicated that HcaA is
241 closest to the HcaA paralog of *H. fennelliae*, but not that of *H. canicola*. *H. fennelliae* is the
242 second most prevalent enterohepatic *Helicobacter* species causing invasive infections in
243 humans. The structural similarity between the HcaA and HcaA paralogs of *H. fennelliae*
244 suggests that HcaA plays a critical role in the pathogenesis of enterohepatic *Helicobacter*
245 species in humans. The results of comparative genomic analyses indicate that *H. cinaedi* is a
246 human-adapted lineage, whereas *H. canicola* is not (21). The acquisition of the RGD motif of
247 HcaA during the evolution of *H. cinaedi* may have contributed to the adaptation of *H. cinaedi*
248 to humans, resulting in a higher isolation rate of *H. cinaedi* from humans compared to other
249 enterohepatic *Helicobacter* species. Further investigation is needed to identify the HcaA-
250 binding target in the host cell.

251 This study identified a novel virulence factor of *H. cinaedi*, HcaA, as an adhesin protein.
252 HcaA plays an essential role in the establishing *H. cinaedi* infection both *in vitro* and *in vivo*
253 and is expected to provide essential data for understanding the pathogenicity of *H. cinaedi*
254 and the pathogenesis of *H. cinaedi* infection in the future.

255

256 **MATERIALS AND METHODS**

257 **Condition of bacterial strains and host cells**

258 *H. cinaedi* (MRY08-1234 and MRY12-0027) strains isolated from the blood of patients
259 with bacteremia in Japan were used throughout the study. The *H. cinaedi* strain was cultured
260 as previously described (27). Briefly, strains were subcultured on Brucella agar (Becton,
261 Dickinson, Franklin Lakes, NJ, USA) with 5% horse blood at 37 °C under microaerobic
262 conditions with hydrogen generated by the gas replacement method using an anaerobic gas

263 mixture (H_2, 10%; CO_2, 10%; and N_2, 80%). For liquid culture, bacteria were suspended in
264 Brucella broth (Becton, Dickinson, Franklin Lakes, NJ) with 10% fetal bovine serum (FBS;
265 NICHIREI), and the culture was incubated for 2 days at 37 °C under microaerobic conditions
266 with hydrogen.

267 Human epithelial colorectal adenocarcinoma cells (Caco-2), human myelomonocyte cell
268 line (U937), human colon cancer cell line (HT29), and mucus-secreting HT29 cells (HT29-
269 MX) were used in this study. Caco-2 was maintained in Eagle's minimum essential medium
270 (EMEM, Sigma Aldrich, USA) containing 2 mM l-glutamine, 1 mM sodium pyruvate, 1.5
271 mg/L sodium bicarbonate, 10 mg/L phenol red, 10% heat-inactivated (56 °C, 30 min) FBS,
272 1% non-essential amino acids. U937, HT29, and HT29-MX cells were maintained in RPMI
273 1640 (Sigma Aldrich) containing 10% heat-inactivated FBS. All media contained an
274 antimicrobial cocktail (penicillin-streptomycin), except for the *H. cinaedi* infection
275 experiments. All cells were incubated in a 5% CO_2, humidified atmosphere at 37 °C.

276

277 **Generation of deletion mutants of *hcaA* gene in *H. cinaedi***

278 Knockout mutants were generated by paralog recombination according to previously
279 described methods (27). Briefly, 1,000 base pairs of DNA sequences upstream and
280 downstream of *hcaA* gene were PCR-amplified. The primers Upstream-R and Downstream-F
281 contained a linker sequence that overlapped with *aphA* gene. To obtain the construct of *aphA*
282 sandwiched by the target gene sequence (donor fragment), three purified PCR products, up-
283 and downstream of *hcaA* and *aphA*, were mixed and amplified using the Upstream-F and
284 Downstream-R primers. The donor fragment was electroporated into *H. cinaedi* MRY08-1234
285 or MRY12-0027. The transformed *H. cinaedi* was spread onto agar plates containing 10
286 μg/mL kanamycin and 3% agar. After incubation, the growing colonies were selected as
287 knockout mutants. Knockout of *hcaA* was confirmed by PCR and immunoblot analysis.

288 Primers used for cloning and PCR are listed in Table S1. For the immunoblot analysis, whole
289 bacterial cell lysates, culture supernatant, soluble fraction, and membrane fraction were
290 prepared as follows: bacterial culture was incubated until an optical density at 600 nm
291 (OD600) of 0.4 and the supernatant was collected by centrifugation (8,600 × *g*, 10 min, 4 °C).
292 The pellet was resuspended and washed by phosphate-buffered saline (PBS). Then, samples
293 for the analysis were prepared by extracting proteins from the bacterial cells using,
294 EzBactYeast Crusher (ATTO Corp., Tokyo, Japan). The concentration of the extracted
295 protein was measured using the BCA protein assay kit (Thermo Fisher Scientific K.K., Tokyo,
296 Japan). These samples were adjusted to a concentration of 0.5 mg/mL by PBS and separated
297 by 5–20% sodium dodecyl sulfate-polyacrylamide gel electrophoresis (SDS-PAGE), and the
298 separated proteins were transferred to Immobilon™ -FL PVDF (pore size, 0.45 um; Millipore
299 Inc., Burlington, MA, USA) using a semidry electroblotting system (ATTO, Tokyo, Japan).
300 Anti-HcaA antibody was obtained by immunization of rabbits with KLH-conjugated peptide
301 (RGDMPQESKTLEQN corresponding to positions 348–361 of HcaA in MRY08-1234),
302 followed by affinity purification against the peptide. The obtained HcaA rabbit polyclonal
303 antibody was used as the primary antibody for immunoblot analysis (1:1,000), and peroxidase
304 AffiniPure donkey anti-mouse IgG (H+L) (Jackson ImmunoResearch Inc., 1:50,000) were
305 used as secondary antibodies. The bands were visualized using ECL Select (Amersham
306 Biosciences, Amersham, UK) and Amersham™ ImageQuant 800 (Amersham Biosciences).
307

308 **Cell infection experiments**

309 *H. cinaedi* strains were grown for three days in Brucella broth with 10% FBS at 37 °C
310 under microaerobic conditions. After incubation, the bacterial culture was inoculated in 10
311 mL of fresh broth, and the culture was incubated until an OD600 of 0.4. Bacterial cells were
312 harvested by centrifugation (3,350 × *g*, 10 min, 25 °C) and resuspended in a suitable medium

313 for each cell. Infections were performed at a multiplicity of infection (MOI) of 100.
314 Immediately after addition of bacteria, the plates were centrifuged for 5 min at 300 × *g* at
315 25 °C, followed by incubation in 5% CO_2 humidified atmosphere, at 37 °C for 24 h.

316 Cytotoxicity was assessed by measuring lactate dehydrogenase (LDH release assay) using
317 the Cytotoxicity LDH Assay Kit-WST (Dojindo Laboratories, Tokyo, Japan). The assay was
318 performed according to the manufacturer's instructions. Caco-2, HT29, and HT29-MX cells
319 were used in this assay.

320 Cell adhesion and invasive ability were assessed using a gentamicin assay. To evaluate
321 adhesion ability, cells were liberated by trypsinization, seeded into 24-well microtiter plates
322 with tissue-culture-treated polystyrene, flat-bottom (FALCON), and incubated for confluency.
323 Caco-2 cells were infected by adding 1 mL of bacterial suspension (MOI 100) directly to each
324 well. After 4 h of incubation, the non-bound bacteria were removed by washing three times
325 with pre-warmed PBS. To evaluate invasive ability, *H. cinaedi* adherent to Caco-2 cells was
326 incubated in EMEM with gentamicin at 250 μg/mL. After 1.5 h, the infected cells were
327 washed thrice with pre-warmed PBS. In both assays, host cells were washed with PBS
328 containing 0.1% saponin (FUJIFILM). Serial dilutions of the suspension were plated onto
329 Brucella agar containing 5% horse blood and 3% agar (Becton Dickinson, Franklin Lakes, NJ,
330 USA). After incubation, the number of colonies was counted, and the adhesion rate (%) and
331 invasion rate (%) were calculated by dividing the number of adherents and invading bacterial
332 cells by the total number of infected bacterial cells, respectively. The invasion rate of adherent
333 bacteria (%) was calculated by dividing the number of invading bacterial cells by the number
334 of adherent bacterial cells.

335

336 **Animal experiment designs and infection**

337 Six-week-old C57BL/6 female mice maintained under specific pathogen-free conditions

338 (Japan SLC, Inc., Shizuoka, Japan) were used in this study. The mice were fed a standard
339 rodent diet, provided with water ad libitum, housed in microisolator cages, and isolated from
340 specific pathogens.

341 Strains were suspended into PBS became 1×10^9 cells/mL. Then, mice were orally
342 administered 0.2 mL of each bacterial suspension by a 1 mL syringe attached to an oral sonde,
343 every other day for total of three times. As a negative control, the mice were administered the
344 same volume of PBS. The experiment used 14 mice in the control group, 15 mice in the wild-
345 type *H. cinaedi* MRY08-1234 infection group, and 16 mice in the *hcaA*-knockout strain
346 infection group. They were kept in cages with five or six mice.

347 On days 7, 14, and 28 after inoculation, five or six mice from each group were sacrificed
348 for analysis. Serum, cecal content, colon, biceps femoris muscle, trapezius muscle, and heart
349 were collected aseptically for further analysis. All animal experiments and the study protocol
350 were conducted with the approval of the Committee for Animal Experimentation of the
351 National Institute of Infectious Diseases (Acceptance number 121126).

352

353 **ELISA assay**

354 To measure antibody titers against *H. cinaedi* in mouse serum, an enzyme-linked
355 immunosorbent assay (ELISA) was performed as previously described (28). Serum was
356 prepared as follows: whole blood collected during autopsy was incubated at 4 °C and then
357 centrifuged at 2,000 × *g* for 5 min at 4 °C. The supernatant was collected and designated as
358 serum. Serum was mixed with glycerol (50% final concentration) and stored at −20 °C until
359 use. To prepare whole-cell lysates, *H. cinaedi* MRY08-1234 cells were collected, washed
360 twice, and suspended in PBS. The cells were then disrupted by sonication with a Bioruptor II
361 (BMBio, Tokyo, Japan). Each well of Nunc-Immuno 96-well microtiter plates (No. 439454;
362 Thermo Fisher Scientific, Waltham, MA, USA) was coated with 100 μl of whole-cell lysates

363 of *H. cinaedi* MRY08-1234 (4 ug/mL in 0.1 M carbonate/bicarbonate buffer, pH 9.4). After
364 overnight incubation at 4°C, plate washed three times with PBS containing 0.05% (vol/vol)
365 Tween 20 (PBS-T), the wells were saturated with 200 µL of blocking buffer (PBS containing
366 1% BSA) and incubated for 1 h at 37°C while shaking at 500 rpm. After the three times of
367 washing with PBS-T, the wells were filled with 50 µL of serum samples were diluted 100-
368 fold with a blocking buffer (PBS containing 1% BSA), and the plates were incubated for 1 h
369 at 37 °C while shaking at 500 rpm. Horseradish peroxidase (HRP)-conjugated goat anti-
370 mouse IgG secondary antibody (Jackson, Bar Harbor, ME, USA) diluted 5,000-fold in
371 blocking buffer was used. Absorbance at 450 nm (reference wavelength, 620 nm) was
372 measured using a Multiskan FC microplate reader (Thermo Scientific, Waltham, MA, USA).
373

374 **Isolation and detection of *H. cinaedi* from infected mice**

375 Culture and PCR were used to evaluate *H. cinaedi* infection in each organ. For cultivation
376 of *H. cinaedi*, agar plates containing Skirrow (Oxoid), 5% horse blood, 3% agar, and 4 µg/mL
377 ciprofloxacin (FUJIFILM Wako Pure Chemical Co.) were inoculated with cecal contents,
378 colon, biceps femoris muscle, trapezius muscle, and heart that had been homogenized in 300
379 µL of Brucella broth. Since MRY08-1234 is resistant to ciprofloxacin, ciprofloxacin was
380 added to eliminate indigenous intestinal bacteria in mice and isolate only *H. cinaedi*. The
381 plates were incubated at 37 °C under microaerobic conditions for 7 days. The growth of the
382 colonies was confirmed by the detection of *cdt* genes using PCR. The primers used are listed
383 in Table S2. Two, we assessed using genome DNA (gDNA) of *H. cinaedi*. gDNA was
384 extracted using the QIAamp PowerFecal Pro DNA Kit (QIAGEN) for cecal contents, and the
385 remaining tissue was extracted using the DNeasy Blood and Tissue Kit (QIAGEN). The
386 extracted genomic DNA was used for quantitative real-time PCR (qPCR). qPCR was
387 performed using THUNDERBIRD™ SYBR qPCR MIX (Toyobo) and Applied Biosystems®

388 7500Fast (Thermo Fisher Scientific). The primers used are listed in Table S2. To quantify
389 bacterial colonization, correlation curves between Ct and log_{10} CFU/mL were generated. This
390 correlation was used to transform Ct values into log_{10} CFU/g of cecal content.
391
392 **Histology, microscopy, and Fluorescence intensity quantification**
393 Colons from two mice in each group were collected and fixed with a 4% paraformaldehyde
394 phosphate buffer solution (FUJIFILM Wako Pure Chemical Co.). The sections obtained from
395 fixed samples were permeabilized and incubated with anti-*H. cinaedi* antibody (1:1,000) as
396 the first antibody at room temperature for 1 h. Anti-*H. cinaedi* antibody was obtained by
397 immunizing rabbits with heat-inactivated *H. cinaedi* MRY08-1234 as an antigen, followed by
398 protein A-purification. The sections were then rinsed and stained with Alexa Fluor 488 (*H.*
399 *cinaedi*) and 4',6-diamidino-2-phenylindole (DAPI, nuclei). The fluorescence signals were
400 visualized using a laser scanning confocal microscope (Olympus FV3000, Olympus, Tokyo,
401 Japan).
402
403 **HcaA purification**
404 To create recombinant HcaA, we constructed expression vectors: *hcaA* was amplified by
405 PCR and introduced into pCold™ I DNA (TaKaRa, Shiga, Japan) using the In-Fusion® HD
406 Cloning Kit. The primers used to generate the fragments are listed in Table S1. Genomic
407 DNA of the *H. cinaedi* strain MRY08-1234 was used to amplify the partial *hcaA* gene. The
408 expression vector containing the partial *hcaA* gene was transferred into *Escherichia coli* BL21
409 (DE3) pLysS cells and spread on LB agar plates containing 100 μg/mL ampicillin. The
410 growing colonies were inoculated into 100 mL of LB broth containing 100 μg/mL ampicillin
411 and incubated at 37 °C with constant shaking at 200 rpm for 3 h. Cells were further
412 transferred into 900 mL of fresh medium grown in a 2 L flask at 37 °C until OD600 of 0.6.

413 Protein expression was induced by cooling in ice water for 1 h and adding 400 μL of 1 mM
414 isopropyl β-d-thiogalactopyranoside (IPTG). Recombinant HcaA was expressed as a fusion
415 protein containing a histidine tag (His). The cell cultures were further incubated for overnight
416 at 15 °C. Bacteria were harvested by centrifugation at 5,000 × *g* for 10 min at 4 °C and
417 resuspended in 10 mL of 20 mM Tris-HCl (Nakarai), 150 mM NaCl (FUJIFILM Wako Pure
418 Chemical Co.), and 40 mM imidazole (FUJIFILM Wako Pure Chemical Co.) at pH 7.6 with
419 protease inhibitor. Suspended solution was sonicated on ice and supernatant was harvested by
420 centrifugation at 5,000 × *g* for 45 min at 4 °C. The recombinant protein was purified in two
421 steps using an affinity column (HisTrap FF crude, Cytiva), followed by size exclusion
422 chromatography (Superdex™ 200 Increase 10/300 GL, Cytiva). To replace the RGD motif of
423 the HcaA protein with RAD, site-directed mutagenesis of the HcaA expression vector was
424 performed using PrimeSTAR® GXL DNA Polymerase and specific primers (Table S1).
425 Purified wild-type and mutant HcaA proteins were verified using SDS-PAGE.
426
427 **Adhesion assay of HcaA protein to U937 cells**
428 Purified HcaA and mutant HcaA were prepared at a concentration of 50 μg/mL in PBS,
429 dispensed 100 uL/well into 96-well plates, and fixed by incubation overnight at 4 °C. This
430 was then washed with pre-warmed PBS; 100 μL of 2% BSA in PBS was added and incubated
431 again overnight at 4 °C (blocking). U937 cells were incubated until confluence and then
432 diluted with MEM to a concentration of 1×10^5 cells/mL. Fluorescein (FUJIFILM Wako) was
433 added to the cell suspension at a final concentration of 1 mg/mL and incubated for 30 min at
434 37 °C. After washing with MEM, MEM containing 2 mM Ca and 2 mM Mg was added and
435 allowed to react for 30 min on ice in the dark. The cell suspension, diluted to a concentration
436 of 5×10^5 /mL, was then dispensed onto plates coated with HcaA and incubated at 37 °C for 1
437 h. After washing and replacement with phenol red-free MEM medium (Sigma), fluorescence

438 was measured, and the number of cells bound to purified proteins was observed.

439

440 **Alignment and phylogenetic analysis of HcaA and HcaA paralogs**

441 Amino acid sequences of HcaA paralogs in other enterohepatic *Helicobacter* species were
442 obtained from the whole genome sequences of *H. bilis* ATCC43879 (Accession No.
443 KI392040), and H. fennelliae MRY12-0050 (Accession No. BSAD00000000), *and H.*
444 *canicola* PAGU1409 (accession no. DRR092854) and *H. canis* CCUG32756 (Accession No.
445 GCF008693005) was obtained from the National Center for Biotechnology Information
446 (NCBI). The passenger regions of the amino acid sequences of the HcaA and HcaA paralogs
447 were aligned using ClustalW ver. 2.1 (29), and visualized using CLC Genomics Workbench
448 Version 22.0.1 (QIAGEN). A phylogenetic tree using the aligned amino acid sequences of the
449 passenger domain of HcaA and HcaA paralogs was constructed using RAxML-NG v1.1.0
450 (https://github.com/amkozlov/raxml-ng) and visualized using MEGA X v 10.2.6 (30).

451

452 **Prediction of HcaA structure**

453 Three-dimensional structures of the HcaA sequences from *H. cinaedi* MRY08-1234 were
454 predicted using AlphaFold2 Ver.2.2.2 on the supercomputer system of the Institute for
455 Chemical Research, Kyoto University, with a full dBs preset. Of the five models generated,
456 the ranked zero model was used in this study. Visualization of the predicted structure was
457 performed using PyMOL Molecular Graphics System Ver. 2.2.5.

458

459 **Statistical analysis**

460 Differences in the recovery of *H. cinaedi* by culture from infected mice were analyzed
461 using Fisher's exact test. For other experiments, the Mann–Whitney test was used for
462 comparison. All statistical analyses were performed using GraphPad Prism version 9.4.1 and

were considered statistically significant when the *P* value was < 0.05.

ACKNOWLEDGMENTS

This work was supported by JSPS KAKENHI Grant Numbers 16K18928, 19K07074 (E. R.) and 22K15465 (S. A.), the GSK Japan Research Grant 2017 (E. R.) and by AMED JP20fk0108148 (E. R.).

CONFLICT OF INTEREST

The authors declare no conflicts of interest.

472 **References**

473 1. Polk DB, Peek RM. 2010. *Helicobacter pylori*: gastric cancer and beyond. 6. Nat Rev
474 Cancer 10:403–414. https://doi.org/10.1038/nrc2857.

475 2. Matsuo T, Mori N, Mizuno A, Sakurai A, Kawai F, Starkey J, Ohkushi D, Abe K,
476 Yamasaki M, Ito J, Yoshino K, Mikami Y, Uehara Y, Furukawa K. 2020. Infected aortic
477 aneurysm caused by *Helicobacter cinaedi*: case series and systematic review of the
478 literature. BMC Infect Dis 20:854. https://doi.org/10.1186/s12879-020-05582-7.

479 3. Akiyama T, Imamura H, Fukui N, Sakai N. 2021. *Helicobacter cinaedi*-infected chronic
480 subdural hematoma mimicking an expanding hematoma: A case report. Surg Neurol Int
481 12:288. https://doi.org/10.25259/SNI_387_2021.

482 4. Kawamura Y, Tomida J, Morita Y, Fujii S, Okamoto T, Akaike T. 2014. Clinical and
483 bacteriological characteristics of *Helicobacter cinaedi* infection. Journal of Infection and
484 Chemotherapy 20:517–526. https://doi.org/10.1016/j.jiac.2014.06.007.

485 5. Suzuki T, Kutsuna S, Tsuboi M, Ota M, Hayakawa K, Ohmagari N. 2019. *Helicobacter*
486 *cinaedi* Hepatic Cyst Infection with Bacteremia. Emerg Infect Dis 25:603–604.
487 https://doi.org/10.3201/eid2503.180936.

488 6. Saito J, Rimbara E, Inaguma S, Hasegawa C, Kamiya S, Mizuno A, Sone Y, Ogawa T,
489 Numata Y, Takahashi S, Asano M. 2022. Determining Infected Aortic Aneurysm
490 Treatment Using Focused Detection of *Helicobacter cinaedi*. Emerg Infect Dis 28:1494–
491 1498. https://doi.org/10.3201/eid2807.212505.

492 7. Totten PA, Fennell CL, Tenover FC, Wezenberg JM, Perine PL, Stamm WE, Holmes
493 KK. 1985. *Campylobacter cinaedi* (sp. nov.) and *Campylobacter fennelliae* (sp, nov.):
494 Two New *Campylobacter* Species Associated with Enteric Disease in Homosexual Men.

495 The Journal of Infectious Diseases 151:131–139.
496 https://doi.org/10.1093/infdis/151.1.131.

497 8. Murakami H, Iwata M, Goto M, Takahashi T, Ono E, Sawabe E, Okuzumi K,
498 Yamaguchi K, Takahashi T. 2003. Isolation of *Helicobacter cinaedi* from blood of an
499 immunocompromised patient in Japan. Journal of Infection and Chemotherapy 9:344–
500 347. https://doi.org/10.1007/s10156-003-0265-3.

501 9. Holst H, Andresen K, Blom J, Højlyng N, Kemp M, Krogfelt KA, Christensen JJ. 2008.
502 A Case of *Helicobacter cinaedi* Bacteraemia in a Previously Healthy Person with
503 Cellulitis. Open Microbiol J 2:29–31. https://doi.org/10.2174/1874285800802010029.

504 10. Nielsen HL, Prag J, Krogfelt KA. 2015. *Helicobacter cinaedi* knee infection after
505 arthroscopy in an immunocompetent patient. BMJ Case Rep 2015:bcr2014208637.
506 https://doi.org/10.1136/bcr-2014-208637.

507 11. Araoka H, Baba M, Kimura M, Abe M, Inagawa H, Yoneyama A. 2014. Clinical
508 Characteristics of Bacteremia Caused by *Helicobacter cinaedi* and Time Required for
509 Blood Cultures To Become Positive. Journal of Clinical Microbiology 52:1519–1522.

510 12. Taylor NS, Ge Z, Shen Z, Dewhirst FE, Fox JG. 2003. Cytolethal Distending Toxin: A
511 Potential Virulence Factor for *Helicobacter cinaedi*. The Journal of Infectious Diseases
512 188:1892–1897.

513 13. Scuron MD, Boesze-Battaglia K, Dlakić M, Shenker BJ. 2016. The Cytolethal
514 Distending Toxin Contributes to Microbial Virulence and Disease Pathogenesis by
515 Acting As a Tri-Perditious Toxin. Frontiers in Cellular and Infection Microbiology 6.

516 14. D'Elios MM, Vallese F, Capitani N, Benagiano M, Bernardini ML, Rossi M, Rossi GP,

517 Ferrari M, Baldari CT, Zanotti G, de Bernard M, Codolo G. 2017. The *Helicobacter*
518 *cinaedi* antigen CAIP participates in atherosclerotic inflammation by promoting the
519 differentiation of macrophages in foam cells. Sci Rep 7:40515.
520 https://doi.org/10.1038/srep40515.

521 15. Meuskens I, Saragliadis A, Leo JC, Linke D. 2019. Type V Secretion Systems: An
522 Overview of Passenger Domain Functions. Frontiers in Microbiology 10.

523 16. Palframan S, Kwok T, Gabriel K. 2012. Vacuolating cytotoxin A (VacA), a key toxin for
524 *Helicobacter pylori* pathogenesis. Frontiers in Cellular and Infection Microbiology 2.

525 17. Radin JN, Gaddy JA, González-Rivera C, Loh JT, Algood HMS, Cover TL. 2013.
526 Flagellar Localization of a *Helicobacter pylori* Autotransporter Protein. mBio 4:e00613-
527 12. https://doi.org/10.1128/mBio.00613-12.

528 18. Taniguchi T, Yamazaki W, Saeki Y, Takajo I, Okayama A, Hayashi T, Misawa N. 2016.
529 The pathogenic potential of *Helicobacter cinaedi* isolated from non-human sources:
530 adherence, invasion and translocation ability in polarized intestinal epithelial Caco-2
531 cells in vitro. J Vet Med Sci 78:627–632. https://doi.org/10.1292/jvms.15-0595.

532 19. Flahou B, Haesebrouck F, Smet A, Yonezawa H, Osaki T, Kamiya S. 2013. Gastric and
533 Enterohepatic Non-*Helicobacter pylori* Helicobacters. Helicobacter 18:66–72.
534 https://doi.org/10.1111/hel.12072.

535 20. Saito S, Tsukahara M, Ohkusu K, Kurai H. 2016. *Helicobacter fennelliae* Bacteremia.
536 Medicine (Baltimore) 95:e3556. https://doi.org/10.1097/MD.0000000000003556.

537 21. Gotoh Y, Atsuta Y, Taniguchi T, Nishida R, Nakamura K, Ogura Y, Misawa N, Hayashi
538 T 2022. *Helicobacter cinaedi* is a human-adapted lineage in the *Helicobacter*

539 *cinaedi/canicola/'magdeburgensis'* complex. Microbial Genomics 8:000830.
540 https://doi.org/10.1099/mgen.0.000830.

541 22. Matsumoto T, Goto M, Murakami H, Tanaka T, Nishiyama H, Ono E, Okada C, Sawabe
542 E, Yagoshi M, Yoneyama A, Okuzumi K, Tateda K, Misawa N, Yamaguchi K. 2007.
543 Multicenter Study To Evaluate Bloodstream Infection by *Helicobacter cinaedi* in Japan.
544 J Clin Microbiol 45:2853–2857. https://doi.org/10.1128/JCM.00465-07.

545 23. Aricò B, Nuti S, Scarlato V, Rappuoli R. 1993. Adhesion of *Bordetella pertussis* to
546 eukaryotic cells requires a time-dependent export and maturation of filamentous
547 hemagglutinin. Proceedings of the National Academy of Sciences 90:9204–9208.
548 https://doi.org/10.1073/pnas.90.19.9204.

549 24. Dautin N. 2010. Serine Protease Autotransporters of *Enterobacteriaceae* (SPATEs):
550 Biogenesis and Function. 6. Toxins 2:1179–1206. https://doi.org/10.3390/toxins2061179.

551 25. Sause WE, Castillo AR, Ottemann KM. 2012. The *Helicobacter pylori* Autotransporter
552 ImaA (HP0289) Modulates the Immune Response and Contributes to Host Colonization.
553 Infect Immun 80:2286–2296. https://doi.org/10.1128/IAI.00312-12.

554 26. Guignot J, Segura A, Nhieu GTV. 2015. The Serine Protease EspC from
555 Enteropathogenic *Escherichia coli* Regulates Pore Formation and Cytotoxicity Mediated
556 by the Type III Secretion System. PLOS Pathogens 11:e1005013.
557 https://doi.org/10.1371/journal.ppat.1005013.

558 27. Rimbara E, Mori S, Kim H, Suzuki M, Shibayama K. 2018. Mutations in Genes
559 Encoding Penicillin-Binding Proteins and Efflux Pumps Play a Role in β-Lactam
560 Resistance in *Helicobacter cinaedi*. Antimicrobial Agents and Chemotherapy
561 62:e02036-17. https://doi.org/10.1128/AAC.02036-17.

562 28. Matsui H, Suzuki M, Isshiki Y, Kodama C, Eguchi M, Kikuchi Y, Motokawa K, Takaya
563 A, Tomoyasu T, Yamamoto T. 2003. Oral Immunization with ATP-Dependent Protease-
564 Deficient Mutants Protects Mice against Subsequent Oral Challenge with Virulent
565 Salmonella enterica Serovar Typhimurium. Infection and Immunity 71:30–39.
566 https://doi.org/10.1128/IAI.71.1.30-39.2003.

567 29. Larkin MA, Blackshields G, Brown NP, Chenna R, McGettigan PA, McWilliam H,
568 Valentin F, Wallace IM, Wilm A, Lopez R, Thompson JD, Gibson TJ, Higgins DG.
569 2007. Clustal W and Clustal X version 2.0. Bioinformatics 23:2947–2948.
570 https://doi.org/10.1093/bioinformatics/btm404.

571 30. Kumar S, Stecher G, Li M, Knyaz C, Tamura K. 2018. MEGA X: Molecular
572 Evolutionary Genetics Analysis across Computing Platforms. Mol Biol Evol 35:1547–
573 1549. https://doi.org/10.1093/molbev/msy096.

574

575 **Table and figure legends**

Table 1. Recovery of *H. cinaedi* from tissues of *H. cinaedi*-infected mice

	No. of positive samples/no. of mice tested*					
	Post-infection (days)					
	7		14		28	
Tissue	WT	KO	WT	KO	WT	KO
Heart	0/5	0/6	0/5	0/5	0/5	0/5
Biceps femoris muscle	1/5	0/6	0/5	0/5	1/5	0/5
Trapezius muscle	0/5	0/6	0/5	0/5	0/5	0/5
Colon	1/5	0/6	1/5	1/5	1/5	0/5
Cecal contents	4/5[†]	0/6	2/5	1/5	0/5	2/5

* Numerator is the number of mice positive for *H. cinaedi* by culture; denominator is the total number of mice sampled. [†] Significantly different vs. KO by Fisher's extract test (P <0.01). WT, wild type; KO, HcaA-knockout

576

577 **Figure legends**

578 Fig. 1. Construction of *hcaA*-knockout strain.

579 (A) Schematic diagram of the knockout strategy for the *hcaA* gene. The *hcaA* locus on the
580 *H. cinaedi* MRY12-0027 and MRY08-1234 chromosomes, the donor fragment used to disrupt
581 the *hcaA* gene locus, and the predicted *hcaA* gene locus after homologous recombination are
582 shown. (B, C) Confirmation of *hcaA* gene knockout. (B) PCR using genomic DNA from wild
583 type (MRY12-0027 WT and MRY08-1234 WT) and HcaA-knockout (MRY12-0027 Δ*hcaA*
584 and MRY08-1234 Δ*hcaA*) strains as template. Lane 1, MRY12-0027 WT; Lane 2, MRY12-
585 0027 *ΔhcaA*; Lane 3, MRY08-1234 WT; Lane 4, MRY08-1234 *ΔhcaA*; Lane 5, OneSTEP
586 Marker 6 (λ/Sty I digest) (Nippon Gene Co., Ltd.). White arrows indicate amplicons of *hcaA*
587 gene (5,478 bp). The absence of the amplicons in HcaA-knockout strains was confirmed. (C)
588 Immunoblot of HcaA. The upper and bottom panels show MRY12-0027 and MRY08-1234,
589 respectively. Lane M, Precision Plus Protein Dual Color Standards (Bio-Rad); Lane 1 and 5,
590 whole cell lysate; Lane 2 and 6, culture supernatant fraction; Lane 3 and 7, membrane
591 fraction; Lane 4 and 8, soluble fraction. The size of HcaA was expected to be 150 kDa, and a
592 band corresponding to 150 kDa was observed in the WT (lanes 1 and 3) but not in the ΔHcaA
593 strain (lanes 5 and 7), confirming the knockout and localization of HcaA.

594

595 Fig. 2. Knockout of HcaA reduced the cytotoxicity caused by *H. cinaedi* infection and the
596 adherence of *H. cinaedi* to cells.

597 (A) LDH assay for evaluating cytotoxicity. Each cell was infected with wild type (MRY12-
598 0027 WT) and HcaA-knockout (MRY12-0027 ΔHcaA) strains for 24 h (MOI 100).
599 Cytotoxicity (%) was calculated using the method described in the instructions. The results
600 are presented as the mean ± standard deviation (n = 6/group). (B), (C) and (D): Adhesion and
601 invasion assay experiments against Caco-2 cells. Caco-2 infected with wild type (MRY12-

602 0027 WT or MRY08-1234 WT) and HcaA knockout (MRY12-0027 ΔHcaA or MRY08-1234
603 ΔHcaA) strains for 4 h (MOI 100). The adhesion rate (B) and invasion rate (C) were
604 calculated by dividing the number of adherent bacteria cells and invading bacteria cells by the
605 number of total infected bacteria cells, respectively. Invasion rate of adhering bacteria (D)
606 was calculated by dividing the number of invading bacteria cells by the number of adherent
607 bacteria cells. *, $P < 0.05$; ***, $P < 0.001$; ns, not specified.
608
609 Fig. 3. Knockout of HcaA reduced *H. cinaedi* colonization in mice.
610 (A) Schematic of animal experiments. C57BL/6 mice were infected with *H. cinaedi*
611 MRY08-1234 wild type or MRY08-1234 ΔHcaA strains for 28 days after oral administration.
612 The bacteria were inoculated with 0.2 mL of each bacterial suspension (10^9 CFU) every three
613 days for a total of three inoculations. For negative control, the same volume of PBS was
614 inoculated. Cecal contents, colon, biceps femoris muscle, trapezius muscle, heart, and blood
615 were collected and analyzed at days 7, 14, and 28 days, based on the day of the last infection.
616 (B) Measurement of anti-*H. cinaedi* antibody titers in infected mice by ELISA. Sera from
617 mice at 7, 14 and 28 days after inoculation were used. Black squares and gray triangles
618 indicate serum from the group of infected wild type (black square, WT) or HcaA knockout
619 (gray triangle, ΔHcaA) strains, respectively. Means and SD reflect values of five mice per
620 group. **, $P < 0.01$. (C) CFU was estimated by qPCR using DNA obtained from cecal
621 contents of mice infected with wild-type or HcaA-knockout *H. cinaedi* for 7, 14, and 28 days
622 after infection. CFU was calculated the as threshold cycle (Ct) values using a correlation
623 curve between Ct values and CFU/mL, and $\log_{10}$ CFU/gram of cecal contents was used for the
624 comparison. Means and SD reflect values of five mice per group. *, $P < 0.05$; ns, not specified.
625 (D) Representative confocal laser-scanning microscopy images of the colon from *H. cinaedi*-

626 infected mice. Green, *H. cinaedi*; blue, nucleus. Tissues were imaged on an inverted laser
627 scanning fluorescent microscope (Olympus) using a 40× objective lens.
628
629 Fig. 4. The RGD motif on HcaA contributes to the adhesion of *H. cinaedi*.
630 (A) SDS-PAGE of the purified WT HcaA and mutant HcaA, stained with Coomassie brilliant
631 blue (CBB). HcaA (120 kDa) with RGD motif (WT HcaA) and HcaA with glycine replaced
632 with alanine in the RGD motif (Mutant HcaA) were expressed in *E. coli* and purified. Proteins
633 were adjusted to 1 mg/mL concentrations and applied. (B) The adhesion ability of purified
634 HcaA proteins with RGD motif (WT HcaA) and HcaA with RAD motif (Mutant HcaA) to
635 U937 cells. Fluorescent-labeled U937 cells attached to HcaA proteins were compared by
636 measuring the fluorescence at 490 nm. **, $P < 0.01$. (C) Phylogenetic tree constructed from
637 the alignment of the passenger domain of the HcaA and HcaA paralogs. Alignment was
638 performed using ClustalW ver. 2.1. The maximum-likelihood tree was constructed using
639 RAxML (https://github.com/amkozlov/raxml-ng) and visualized using MEGA-X v 10.2.6. A
640 comparison of the amino acid sequence of HcaA around the position on the RGD motif
641 showed that the RGD motif was present only in HcaA of *H. cinaedi* (red text). (D) Three-
642 dimensional structure of HcaA and HcaA paralogs predicted by AlphaFold2. HcaA paralogs
643 of *H. bilis*, *H. fennelliae*, *H. canicola*, and *H. canis* were analyzed and compared. The RGD
644 motif is located at the protrusion in HcaA (inside the square). HcaA paralogs had a structure
645 protruding from the surface like HcaA; however, the protruding structure did not contain the
646 RGD motif.

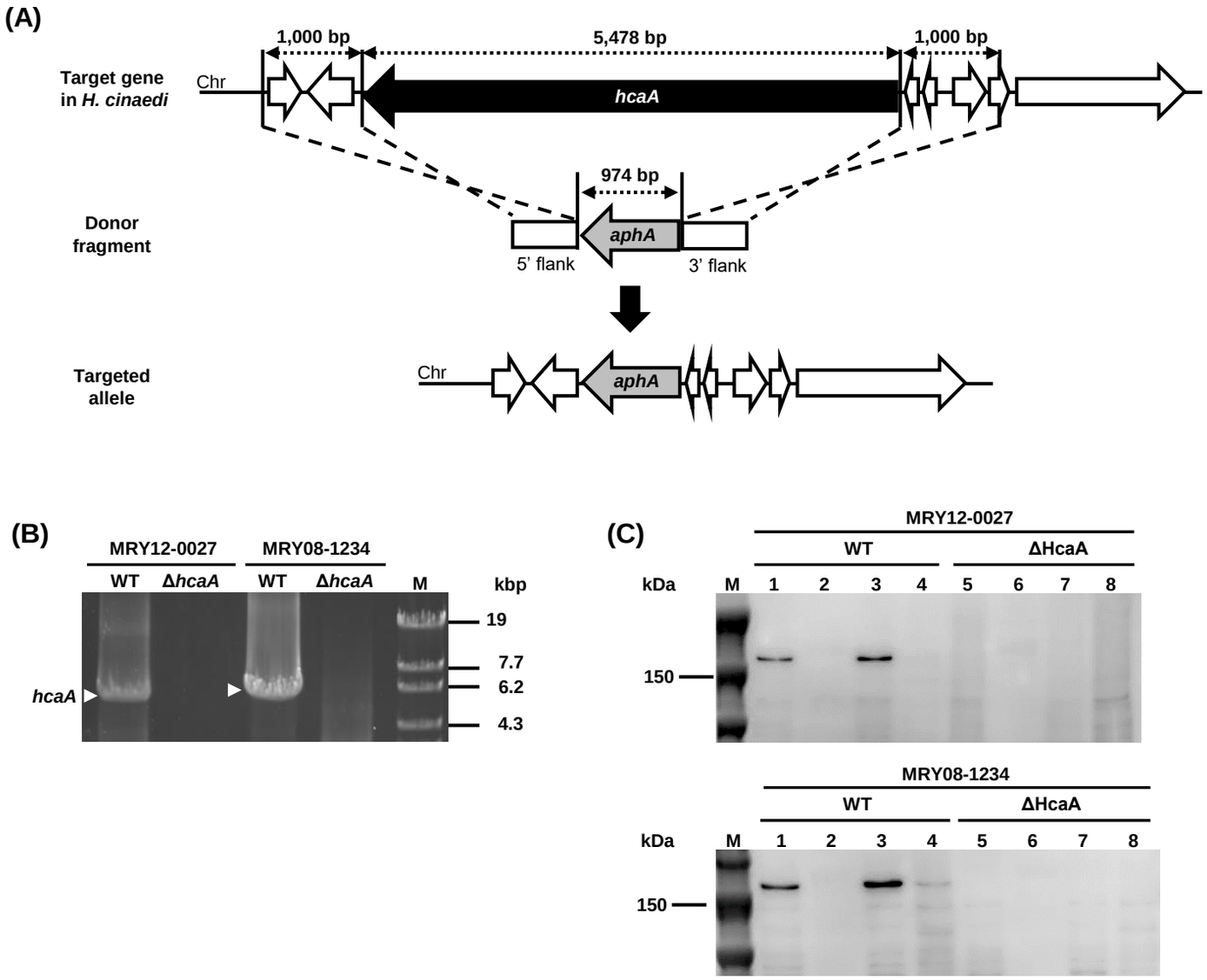
(A)
Target gene in H. cinaedi
Chr
1,000 bp
5,478 bp
1,000 bp
hcaA
Donor fragment
974 bp
aphA
5' flank
3' flank
Targeted allele
Chr
aphA
(B)
MRY12-0027
MRY08-1234
WT
ΔhcaA
WT
ΔhcaA
M
kbp
hcaA
19
7.7
6.2
4.3
(C)
MRY12-0027
WT
ΔHcaA
kDa
M
1
2
3
4
5
6
7
8
150
MRY08-1234
WT
ΔHcaA
kDa
M
1
2
3
4
5
6
7
8
150

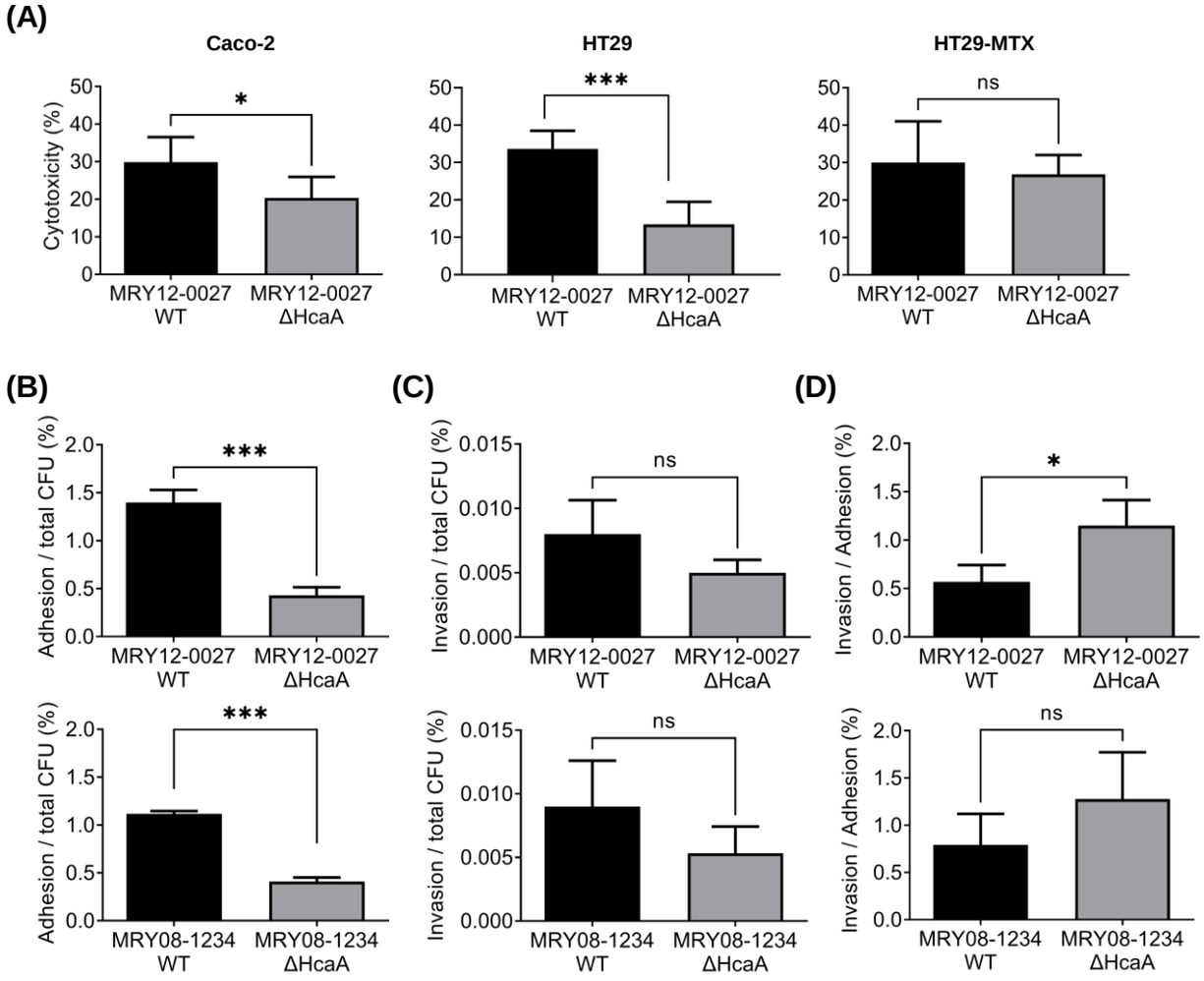
(A)
Caco-2
HT29
HT29-MTX
Cytotoxicity (%)
*
***
ns
MRY12-0027 WT
MRY12-0027 ΔHcaA
(B)
(C)
(D)
Adhesion / total CFU (%)
Invasion / total CFU (%)
Invasion / Adhesion (%)
MRY08-1234 WT
MRY08-1234 ΔHcaA

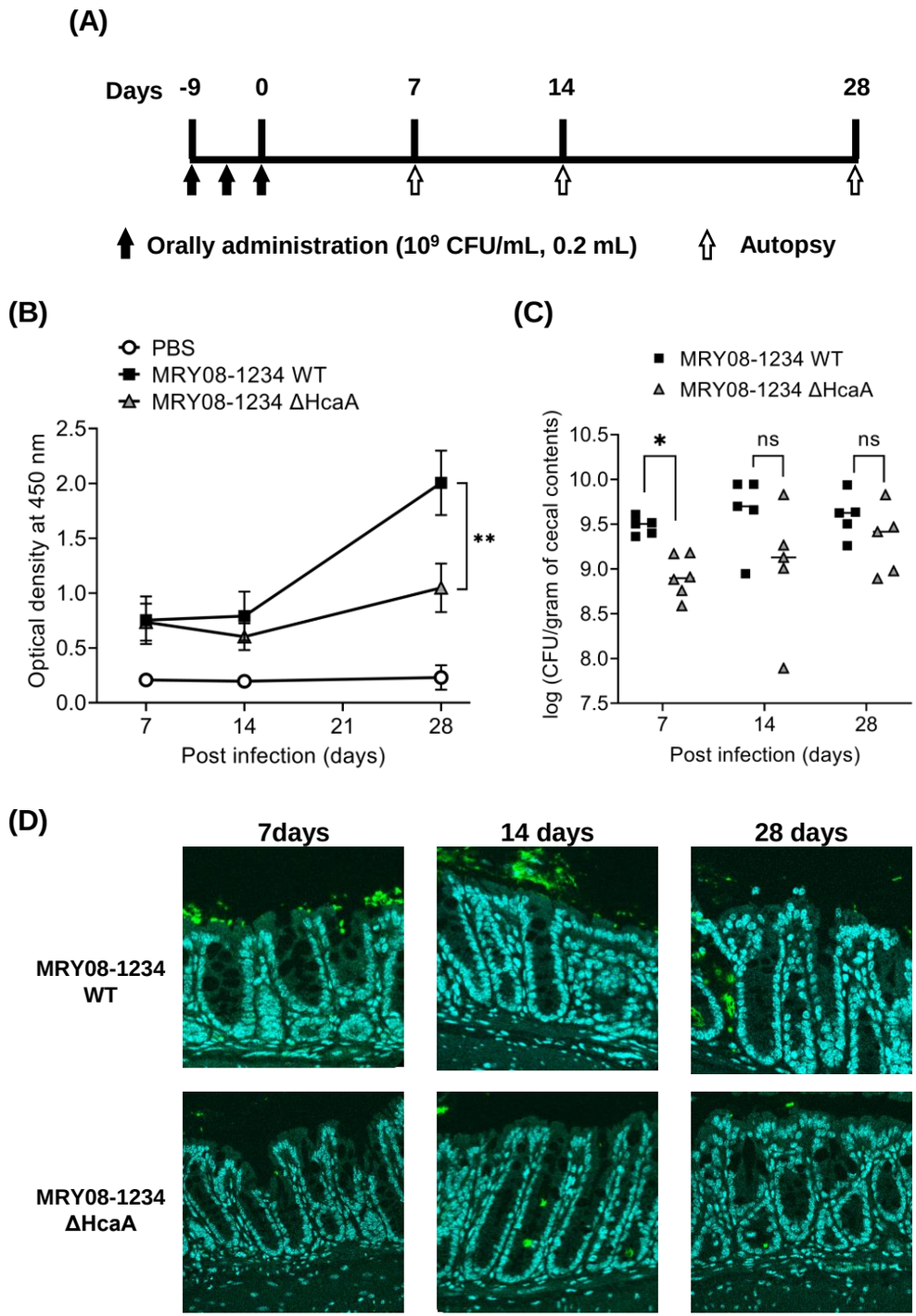
(A)
Days -9 0 7 14 28
Orally administration (10⁹ CFU/mL, 0.2 mL)
Autopsy
(B)
PBS
MRY08-1234 WT
MRY08-1234 ΔHcaA
Optical density at 450 nm
2.5
2.0
1.5
1.0
0.5
0.0
**
7 14 21 28
Post infection (days)
(C)
MRY08-1234 WT
MRY08-1234 ΔHcaA
log (CFU/gram of cecal contents)
10.5
10.0
9.5
9.0
8.5
8.0
7.5
*
ns
ns
7 14 28
Post infection (days)
(D)
7days
14 days
28 days
MRY08-1234 WT
MRY08-1234 ΔHcaA

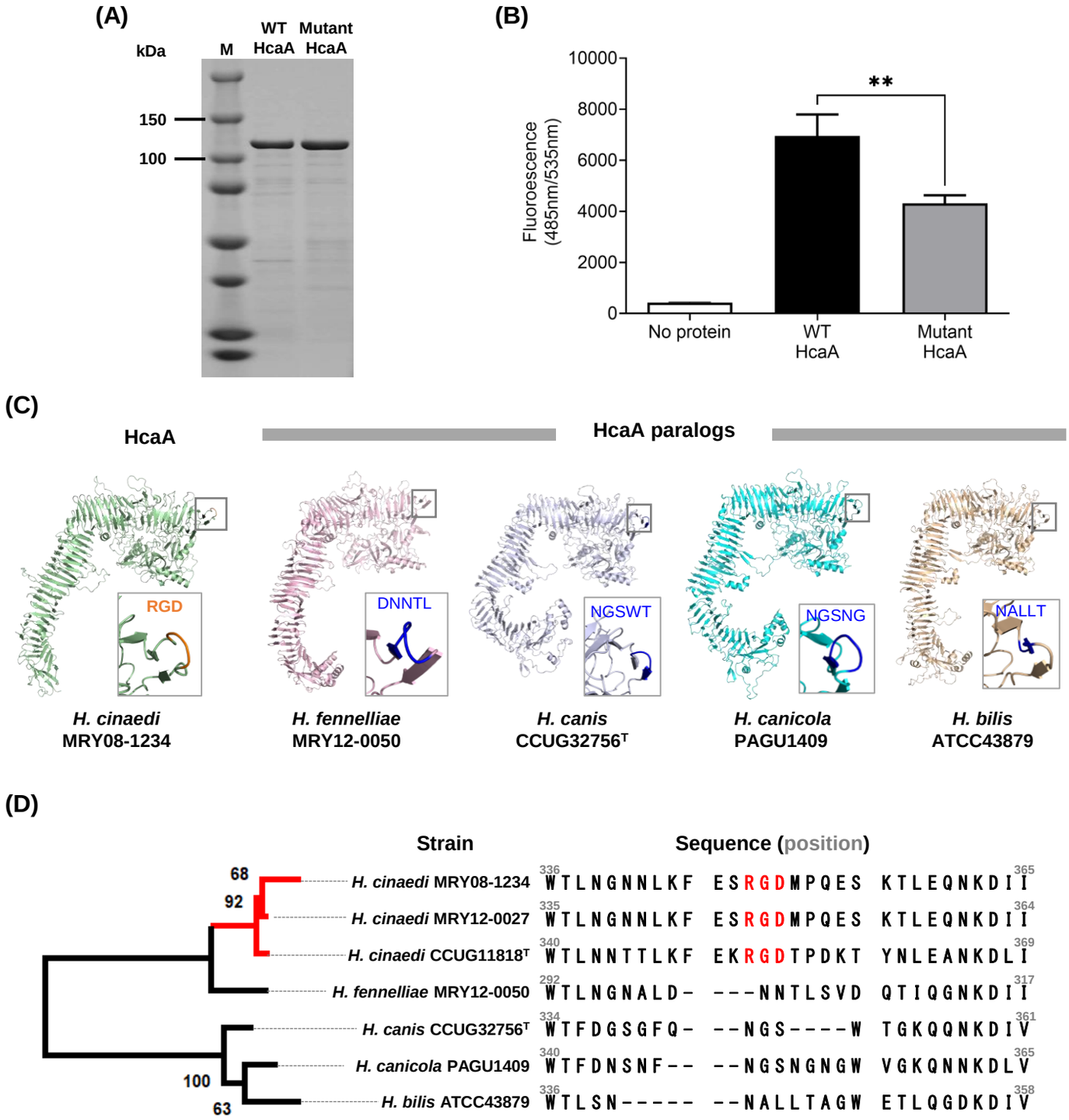
(A)
kDa
M
WT HcaA
Mutant HcaA
150
100
(B)
Fluoroescence (485nm/535nm)
10000
8000
6000
4000
2000
0
**
No protein
WT HcaA
Mutant HcaA
(C)
HcaA
HcaA paralogs
RGD
DNNTL
NGSWT
NGSNG
NALLT
H. cinaedi MRY08-1234
H. fennelliae MRY12-0050
H. canis CCUG32756T
H. canicola PAGU1409
H. bilis ATCC43879
(D)
Strain
Sequence (position)
68
92
100
63
H. cinaedi MRY08-1234 336 WTLNGNNLKF ESRGDMPQES KTLEQNKDII 365
H. cinaedi MRY12-0027 335 WTLNGNNLKF ESRGDMPQES KTLEQNKDII 364
H. cinaedi CCUG11818T 340 WTLNNTTLKF EKRGDTPDKT YNLEANKDLI 369
H. fennelliae MRY12-0050 292 WTLNGNALD- ---NNTLSVD QTIQGNKDII 317
H. canis CCUG32756T 334 WTFDGSGFQ- --NGS----W TGKQQNKDIV 361
H. canicola PAGU1409 340 WTFDNSNF-- --NGSNGNGW VGKQNNKDLV 365
H. bilis ATCC43879 336 WTLSN----- --NALLTAGW ETLQGDKDIV 358